Freeze-Dried Biomolecules: FT-ICR Studies of the Specific Solvation of Functional Groups and Clathrate Formation Observed by the Slow Evaporation of Water from Hydrated Peptides and Model Compounds in the Gas Phase

Sang-Won Lee, Patrick Freivogel, Thomas Schindler, and J. L. Beauchamp*

Contribution from the Beckman Institute, California Institute of Technology, Pasadena, California 91125

Received June 15, 1998

Abstract: Solvent evaporation from extensively hydrated peptides and selected model compounds formed by electrospray ionization has been examined using an external ion source Fourier transform ion cyclotron resonance (FT-ICR) mass spectrometer. Water evaporation from the clusters, formed at room temperature by appropriate operation of an electrospray ion source, is initially rapid and results in evaporative cooling of the clusters to a temperature around 130−150 K, determined by the balance between evaporative cooling and heating by background blackbody radiation. In this "freeze-drying" process, it is observed that the kinetics of solvent evaporation and the cluster size distributions are highly dependent on the nature of the core ion in the cluster. In agreement with earlier studies of the hydrated proton, pure water clusters exhibit special stability characteristic of clathrate formation where, for example, a hydronium ion is encapsulated by a pentagonal dodecahedron of twenty water molecules. Similar clustering of water occurs around protonated primary alkylamines where the protonated amine replaces one of the water molecules in the clathrate structures, which encapsulate one or more neutral water molecules. This observation supports the conjecture that the doubly protonated cyclic decapeptide gramicidin S with 40 water molecules attached, the most significant magic number observed in mass spectra at various delay times, has both protonated ornithine residues solvated by pentagonal dodecahedron clathrate structures. Other peptides such as doubly protonated bradykinin do not exhibit any specific solvation during the freeze-drying process. Studies of model compounds are presented which reveal other interesting aspects of water structure around singly and multiply charged ions with low extents of hydration, including the observation of neutral clathrates attached to a "spectator" ion.

Introduction

Solvated ions in the gas phase are frequently inferred as model systems to bridge the gap between solution and gas-phase chemistry. This expectation has led to wide-ranging investigations of the solvation of small ions in the gas phase and the effect of solvent on reactivity using various techniques, including high-pressure mass spectrometry[1], flow tubes[2], guided ion beam instruments[3], and Fourier transform ion cyclotron resonance (FT-ICR) mass spectrometry.[4,5] Direct structural information on small solvated ions has been obtained by infrared predissociation spectroscopy[6] and by theoretical *ab initio* calculations.[7]

A detailed understanding of the interaction of biomolecules with solvent molecules is of considerable interest in the fields of chemistry and biology. Water is known to be critical in protein folding and maintenance of protein structure.[8] A minimum amount of water is a necessary condition for enzymes to gain their biological activities.[9] X-ray studies of protein crystals show that residual solvent is well-ordered around proteins and has markedly different properties from the bulk solvent.[10]

The capability to generate and investigate solvated biomolecules in the gas phase would have the potential to reveal detailed information on the specific interaction of small numbers of solvent molecules with biomolecules and provide a better understanding of the role of solvent molecules in determining reactivity and structure. Only a few studies of the solvation of peptides in the gas phase have been published. The introduction of electrospray ionization (ESI)[11] has facilitated the production of solvated singly and multiply charged peptides[12] and organic compounds.[13] With the use of high-pressure mass spectrometry, free energies of hydration have been determined for Gly_nH^+, *n*

(1) (a) Kebarle, P.; Tang, L. *Anal. Chem*. **1993**, *68*, 972A. (b) Meot-Ner, M.; Speller, C. V. *J. Phys. Chem.* **1986**, *90*, 6616.
(2) (a) Viggiano, A. A.; Dale, F.; Paulson, J. F. *J. Chem. Phys.* **1988**, *88*, 2469. (b) Castleman, A. W., Jr.; Bowen, K. H. *J. Phys. Chem*. **1996**, *100*, 12911.
(3) (a) Honma, K.; Sunderlin, L. S.; Armentrout, P. B. *Int. J. Mass Spectrom. Ion Processes* **1992**, *117*, 237. (b) Armentrout, P. B.; Baer, T. *J. Phys. Chem.* **1996**, *100*, 12866.
(4) Kofel, P.; McMahon, T. B. *Int. J. Mass Spectrom. Ion Processes* **1990**, *98*, 1.
(5) (a) Schindler, T.; Berg, C.; Niedner-Schatteburg, G.; Bondybey, V. E. *Chem. Phys. Lett.* **1994**, *229*, 57. (b) Schindler, T.; Berg, C.; Niedner-Schatteburg, G.; Bondybey, V. E. *J. Chem. Phys.* **1996**, *104*, 3998.
(6) (a) Yeh, L. I.; Okumura, M.; Myer, J. D.; Price, J. M.; Lee, Y. T. *J. Chem. Phys*. **1989**, *91*, 7319. (b) Cao, Y.; Choi, J.-H.; Haas, B.-M.; Johnson, M. S.; Okumura, M. *J. Chem. Phys*. **1993**, *99*, 9307.
(7) (a) Xantheas, S. S. *J. Phys. Chem*. **1996**, *100*, 9703. (b) Wei, D.; Salahub, D. R. *J. Chem. Phys*. **1997**, *106*, 6086.
(8) Finney, J. L. In *Water, A Comprehensive Treatise*; Franks, F., Ed.; Plenum Press: New York, 1979; Vol. 6, p 47.
(9) (a) Tait, M. J.; Franks, F. *Nature* **1971**, *230*, 91. (b) Rees, D. C.; Lewis, M.; Lipscomb, W. M. *J. Mol. Biol.* **1985**, *168*, 367.
(10) Teeter, M. M. *Annu. Rev. Biophys. Biophys. Chem.* **1991**, *20*, 577.
(11) (a) Yamashita, M.; Fenn, J. B. *J. Phys. Chem.* **1984**, *88*, 4451. (b) Fenn, J. B.; Mann, M.; Meng, C. K.; Wong, S. F.; Whitehouse, C. M. *Science* **1989**, *246*, 64.

10.1021/ja982075x CCC: $15.00
Published on Web 10/30/1998

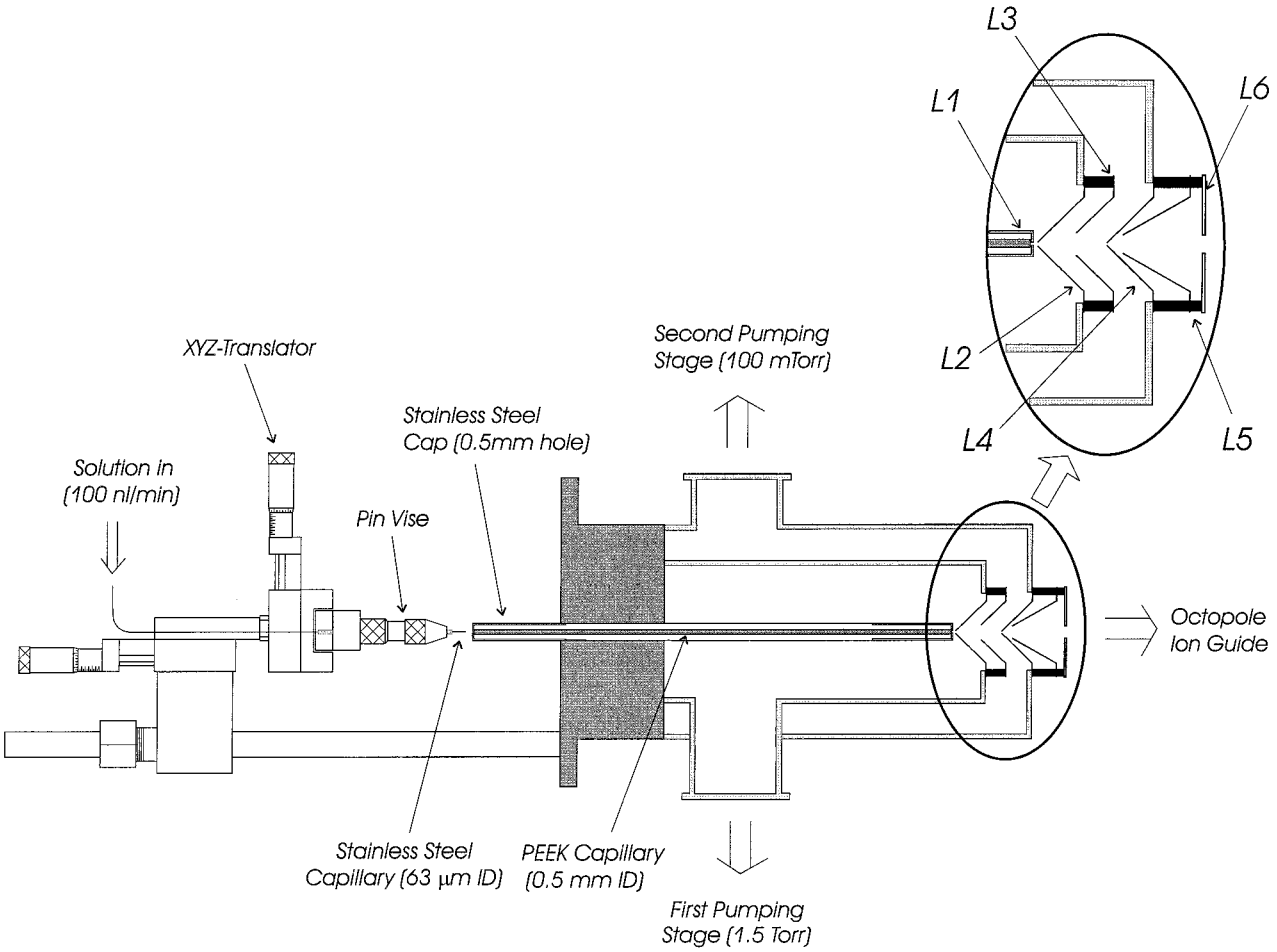

Figure 1. Schematics for the modified electrospray source with the extraction lenses shown in the circle.

$= 1-4$, with the addition of up to four water molecules.[14] With an electrospray ion source coupled to a quadrupole mass spectrometer, the influence of postcapillary collision-induced dissociation (CID) on production of solvent clusters has been investigated.[15] Controlled heating of the desolvation capillary has been used to investigate the effect of temperature on cluster size distributions of solvated biomolecules measured with a quadrupole mass spectrometer.[16] In combined ion mobility−mass spectrometry studies, Jarrold and co-workers have recently demonstrated that the average number of water molecules adsorbed by cytochrome *c* and apomyoglobin by unfolded conformations is substantially less than that by folded ones.[17] They have also reported the free energies associated with adding the first few water molecules to bovine pancreas trypsin inhibitor in an attempt to observe the known solution behavior of this peptide to strongly bind several interior water molecules.[18]

In this paper we report studies of the slow evaporation of solvent from water clusters of biomolecules using FT-ICR techniques for the first time. FT-ICR,[19] with its capabilities of ultrahigh mass resolution, mass selection, and long ion storage times, is ideally suited for studies of the properties, structures, and reaction dynamics of large ions and ionic clusters[4,5] in the gas phase. Slow solvent evaporation reveals the formation of clusters with enhanced stability, generally referred to as magic number clusters. Studies of model compounds demonstrate other important aspects of water structure around singly and multiply charged ions with low extents of hydration. These results are used to interpret evaporation kinetics and cluster size distributions observed for several small peptides.

Experimental Section

All experiments were performed in an external ion source 7T FT-ICR mass spectrometer that has been described in detail elsewhere.[20] Briefly, the instrument is equipped with a radio frequency only octopole ion guide to transfer the ions from the atmospheric pressure ion source into the ICR cell. An electromechanical shutter is located between the ESI source and the octopole to maintain pressures below 10^{-9} Torr at the ICR cell. The shutter was opened for 2 s to allow ions continuously being generated by the ESI source to enter the octopole ion guide. The rf field of the octopole was turned on only during this period of time. Argon collision gas ($\sim$1 ms pulse, 10^{-6} Torr) was introduced to moderate the ion kinetic energy while the ions were travelling through the octopole ion guide and being trapped in the ICR cell. For the production of hydrated peptides, a modified version of a

(12) (a) McLuckey, S. A.; Glish, G. L.; Asano, K. G.; Bartmess, J. E. *Int. J. Mass Spectrom. Ion Processes* **1991**, *109*, 171. (b) Chowdhury, S. K.; Chait, B. T. *Anal. Chem.* **1991**, *63*, 1660.

(13) Nguyen, V. Q.; Chen, X. G.; Yergey, A. L. *J. Am. Soc. Mass Spectrom.* **1997**, *8*, 1175.

(14) Klaasen, J. S.; Blades, A. T.; Kebarle, P. *J. Phys. Chem.* **1995**, *99*, 15509.

(15) Chowdhury, S. K.; Katta, V.; Chait, B. T. *Rapid Commun. Mass Spectrom.* **1990**, *4*, 81.

(16) Rodriguez-Cruz, S. E.; Klassen, J. S.; Williams, E. R. *J. Am. Soc. Mass Spectrom.* **1997**, *8*, 565.

(17) Fye, J. L.; Woenckhaus, J.; Jarrold, M. F. *J. Am. Chem. Soc.* **1998**, *120*, 1327.

(18) Woenckhaus, J.; Hudgins, R. R.; Jarrold, M. F. *J. Am. Chem. Soc.* **1997**, *119*, 9586.

(19) Marshall, A. G.; Verdun, F. R. In *Fourier Transforms in NMR, Optical, and Mass Spectrometry: A User's Handbook*; Elsevier: Amsterdam, 1990.

(20) Rodgers, M. T.; Campbell, S.; Marzluff, E. M.; Beauchamp, J. L. *Int. J. Mass Spectrom. Ion Processes* **1994**, *137*, 121.

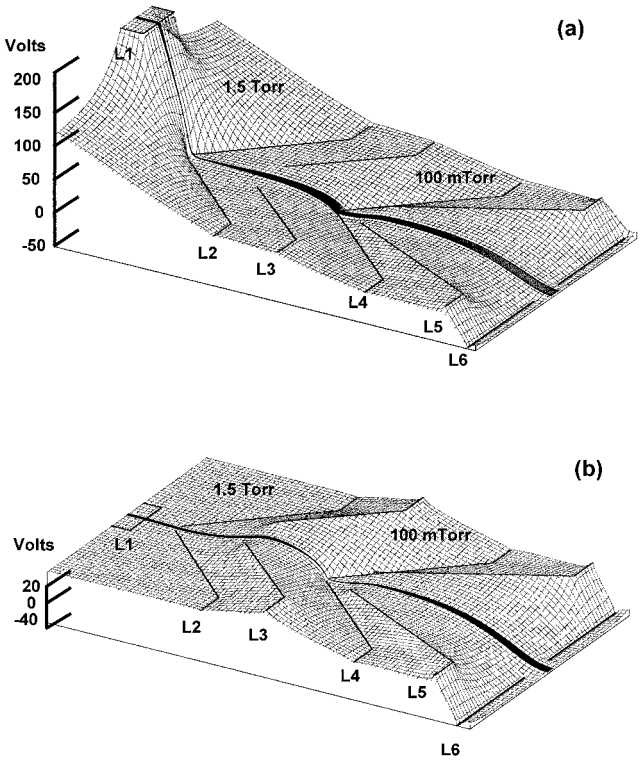

Figure 2. Potential contours of extraction lenses for normal electrospray source (a) and nanoelectrospray source for cluster production (b). "Gentle" sampling of ions is observed to be possible with smooth voltage differences of extraction lenses.

commercially available electrospray ion source (Analytica of Branford, Branford, CT) was used (Figure 1), which will be described in detail elsewhere.[21] A syringe pump (Harvard Apparatus, model 22, South Natick, MA) continuously injects the electrospray solution (0.01% acetic acid in deionized water) through a hypodermic stainless steel needle (63 μm i.d. and 145 μm o.d., Small Parts Inc., Miami Lakes, FL) at a flow rate of 80−150 nl/min. A potential of 1000−2000 V at the entrance cap of the desolvation capillary with the grounded needle initiates sprays. The onset voltage depends on the polarity of the sample solution. The distance between the spray needle and the desolvating capillary is about 2 mm. An *xyz* translator (DAEDAL Inc., Harrison City, PA) allows precise adjustments of the spray needle relative to the entrance cap of the desolvation capillary. The spray was viewed by a microscope at 40-fold magnification (Carl Zeiss, Germany). The same needle can be used for different samples upon changing the solution in a microsyringe. No nebulizer or counterflowing drying gas was used, and the desolvation capillary was operated at room temperature.

Production of hydrated ions is observed to be sensitive to the operation conditions of the electrospray source, especially to voltages on the extraction lenses as shown in the circle of Figure 1. Potential contours and ion trajectory simulations shown in Figure 2 are computed using the SIMION 3D program.[22] Figure 2a shows potential contours for normal electrospray operation with the ion trajectories depicted by lines. A moderately high voltage accelerates ions coming out of the desolvation capillary (L1) to focus them onto the first skimmer. This leads to energetic collisions of the ions with neutrals between L1 and L2, resulting in effective desolvation of hydrated ions. This potential contour would be appropriate for normal ESI operation in which complete desolvation is desired. More gentle sampling of ions can be accomplished with the potentials as shown in Figure 2b. The potential surface between the exit electrode (L1) of the desolvation capillary and the first skimmer (L2) is virtually flat, avoiding energetic ion−neutral collisions in this region of moderate pressure. The ions are focused onto the second skimmer (L4) in a region where the pressure is substantially lower. Extensive ion hydration is observed with these conditions.

(21) Lee, S.-W.; Schindler, T.; Freivogel, P.; Beauchamp, J. L., manuscript in preparation.

(22) Dahl, D. A. SIMION 3D, Version 6.0, Idaho National Engineering Laboratory, Idaho Falls, Idaho, 1995.

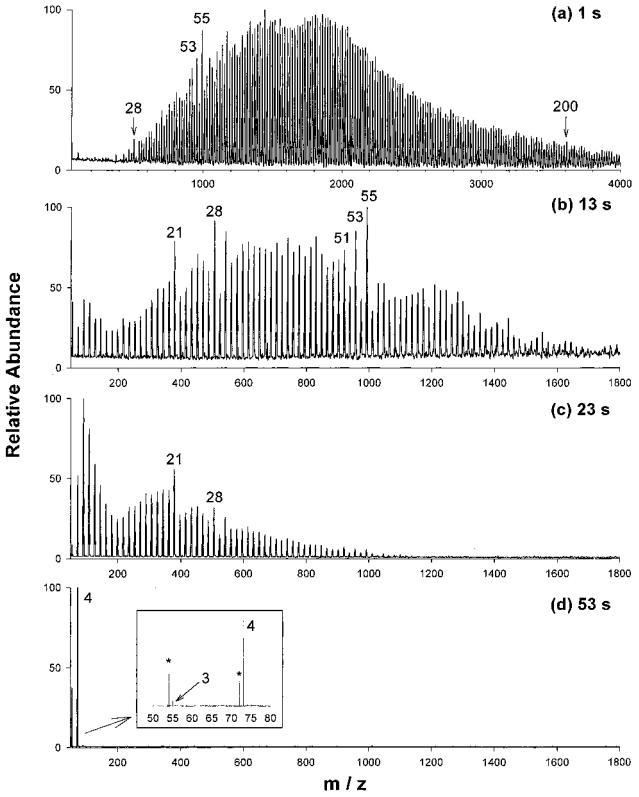

Figure 3. Protonated water clusters detected at various delay times after ion accumulation. Clusters with 21, 28, 51, 53, and 55 water molecules are inferred to have special stability and are referred to as magic numbers. Pure deionized water with a trace amount of acetic acid (0.01%) was used to generate the spectra shown. The asterisks indicate water clusters of an ammonium ion.

Results and Discussion

Protonated Water Clusters. Mass spectra of protonated water clusters taken at various detection delays after ion accumulation are shown in Figure 3. At the shortest delay (1 s, Figure 3a), clusters $H^+(H_2O)_n$ with $n > 200$ are observed. Subsequent evaporation of H_2O occurs on a time scale of 1 min to reduce the clusters to the especially stable hydrated hydronium ion, corresponding to $H^+(H_2O)_4$. Loss of the next water occurs on a time scale of 10 min at ambient temperature. Solvated ions leaving the ESI desolvation capillary are initially equilibrated at ambient temperature. Initial water loss is rapid, leading to evaporative cooling of the clusters. Over the period of observation, the cluster temperature is determined by the balance between evaporative cooling and energy input due to background blackbody infrared radiation. The exchange of energy due to collisions is minimal at the low pressures ($<10^{-9}$ Torr) used in these experiments. The rate of water evaporation is a function of cluster size and, more importantly, temperature. Using the experimental activation parameters for water evaporation from ice, a comparison of calculated rates to our observed evaporation rate indicates that the average cluster temperature is in the temperature range between 130 and 150 K. A more complete analysis with the same conclusion has been reported by Bondybey and co-workers in a FT-ICR study of solvent evaporation from water clusters generated in an external corona discharge ion source[5]. During this "freeze-drying" process, clusters with special stability are identified as prominent features

in the overall cluster distribution. The signature of a stable cluster or magic number is an enhanced abundance accompanied by an unusually low abundance for the cluster with one additional solvent molecule. As also observed by others,[5,23] these magic numbers are discerned for the hydrated proton at $n = 21$, 28, 51, 53, and 55. At long delay times, persistent clusters indicative of special stability may be observed, as in the case of $H^+(H_2O)_4$.

The intricate hydrogen-bonded structures that water can form to solvate and encapsulate both ions and neutrals have been widely investigated for over a century.[24] Two small clathrate structures **1** and **2**, predicted by semiempirical PM3 calcula-

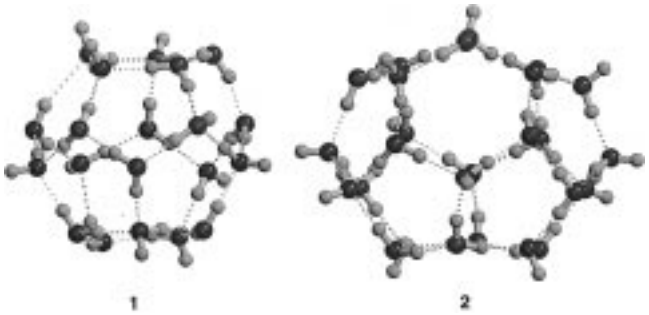

tions,[25] are shown for 20 and 26 water molecules, respectively. Both experimental[23] and theoretical[26] evidence has been offered to support the assignment of the water cluster with $n = 21$ as a clathrate in which 20 waters form a pentagonal dodecahedron structure **1** encapsulating a hydronium ion. Similarly the magic number $n = 28$ can be assigned to the pentakaidecahedron **2** with the larger cavity encapsulating a proton bound dimer of water. Structures for the larger stable clusters with $n = 51$, 53, and 55 are difficult to infer but may comprise more complex clathrates with face-sharing polyhedra that encapsulate varying numbers of neutral and ionic species in cavity voids.

With trace amounts of ammonia present a nearly identical cluster size distribution for $NH_4^+(H_2O)_n$ is observed where magic numbers are discerned at $n = 20$, 27, 50, 52, and 54, suggesting similar encapsulation of the ammonium ion.[23c]

Water Clusters of Singly Protonated Primary Amines. Cluster distributions for protonated *n*-octylamine and 1-adamantylamine after 8 s of evaporation are compared in Figure 4. These primary amines exhibit virtually identical evaporation kinetics and cluster size distributions, with magic numbers at $n = 20$, 27, 50, 52, and 54 for $RNH_3^+(H_2O)_n$. These numbers are 1 less than the magic numbers observed for protonated water clusters. More complete evaporation kinetics are shown for 1-adamantylamine in Figure 5. Nearly identical results are observed in the case of *n*-octylamine. These observations

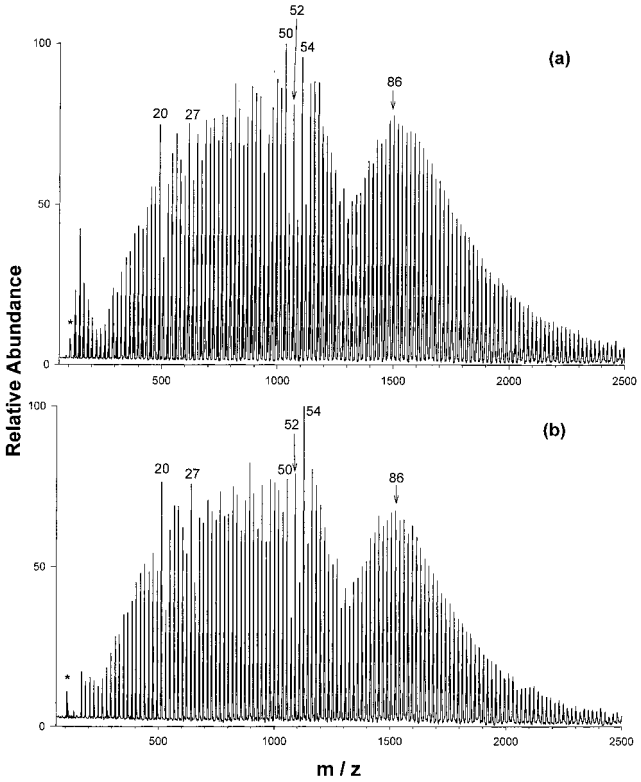

Figure 4. Water clusters of (a) protonated *n*-octylamine, (b) protonated 1-adamantylamine detected at 8 s after ion production. Sample concentrations are approximately 100 μM in 0.01% acetic acid solution. The asterisks indicate protonated water clusters.

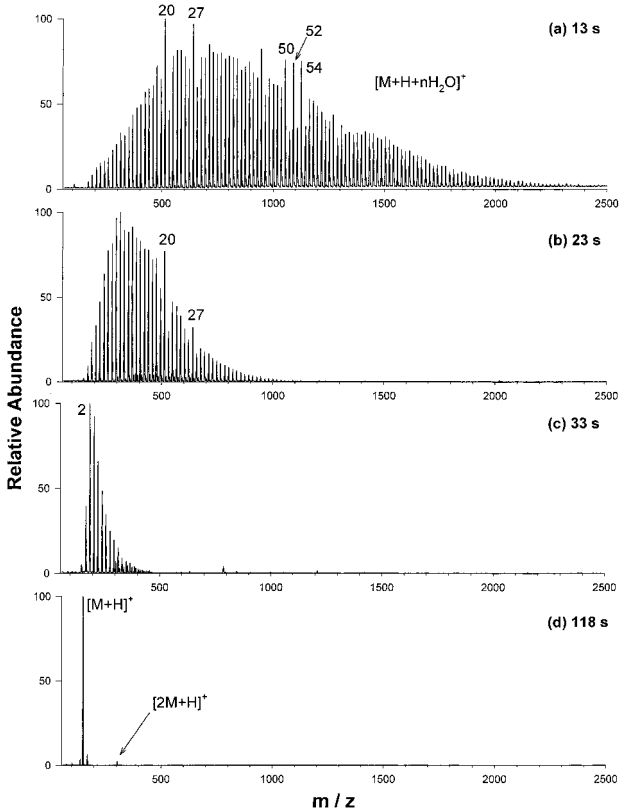

Figure 5. Water clusters of protonated 1-adamantylamine detected at various delay times. Sample concentration is 80 μM in 0.01% acetic acid solution.

suggest that for clusters with fewer than 100 water molecules, solvation is dominated entirely by the protonated amine

(23) (a) Lin, S.-S. *Rev. Sci. Instrum.* **1973**, *44*, 516. (b) Searcy, J. Q.; Fenn, J. B. *J. Chem. Phys.* **1974**, *61*, 5282. (c) Shinohara, H.; Nagashima, U.; Tanaka, H.; Nishi, N. *J. Chem. Phys.* **1985**, *83*, 4184. (d) Wei, S.; Shi, Z.; Castleman, A. W., Jr. *J. Chem. Phys.* **1991**, *94*, 3268.

(24) (a) Jeffrey, G. A. In *Inclusion Compounds*; Atwood, J. L.; Davies, J. E. D.; MacNiol, D. D., Eds.; Academic Press: New York, 1984; Vol. 1, Chapter 5. (b) Lipkowski, J. In *Annual Reports on the Progress of Chemistry Section C*; Webbs, G. A., Eds.; The Royal Society of Chemistry: Cambridge, 1996; Vol. 96, Chapter 10.

(25) Semiempirical calculations at the PM3 level were performed using the Hyperchem computational software package from Hypercube, Inc. PM3 is a preferred semiempirical method in modeling the strengths and energies of hydrogen bonds, giving excellent agreements with ab intio calculations. (a) Zheng, Y.; Merz, K. M. *J. Comput. Chem.* **1992**, *13*, 1151. (b) Jurema, M. W.; Shields, G. C. *J. Comput. Chem.* **1993**, *14*, 89. (c) Campbell, S.; Rodgers, M. T.; Marzluff, E. M.; Beauchamp, J. L. *J. Am. Chem. Soc.* **1995**, *117*, 12840.

(26) (a) Kasser, J. L., Jr.; Hagen, D. E. *J. Chem. Phys.* **1976**, *64*, 1860. (b) Khan, A. *Chem. Phys. Lett.* **1994**, *217*, 443.

functional group and not by the hydrophobic hydrocarbon portion of the molecule. Although protonated *n*-octylamine might insert through an open pentagonal face of the cage structure with the protonated amine moiety replacing the internal hydronium ion, the identical solvation character of protonated 1-adamantylamine suggests that the protonated amino group replaces one of the water molecules in the clathrate structure and that an extra water molecule is encapsulated in the cavity. Semiempirical PM3 calculations predict structure **3** for this

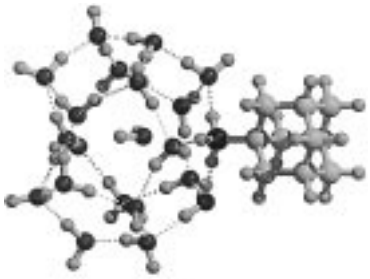

species. Similarly, the cluster with $n = 27$ corresponds to the pentakaidecahedron with the larger cavity accommodating two interior water molecules. The clusters with $n = 50$, 52, 54 may result from face-sharing composite structures in which the protonated primary amine replaces one of the water molecules in the cage structure.

It is of interest to note that a distinctive bimodal distribution of water clusters is observed for the two primary amines in Figure 4a and b, which both have a secondary maximum in the distribution corresponding to 86 water molecules. The remarkable similarity in the water cluster distributions of these two amines even for larger clusters may indicate that a second solvent shell is formed around the charged groups. There are no magic numbers evident in the smooth distributions observed for these larger clusters.

Water Clusters of Doubly Protonated Gramicidin S. Spectra of solvated doubly protonated gramicidin S at various detection delays are shown in Figure 6a−d. Gramicidin S is a compact cyclic decapeptide [(-Pro-Val-Orn-Leu-D-Phe-)$_2$] with hydrophobic residues except for two ornithines with the basic side chain [R = -$(CH_2)_3NH_2$)] where protonation occurs. The distribution of cluster sizes for this peptide is very complex and exhibits magic numbers at $n = 8$, 11, 14, and 40 during solvent evaporation. On the basis of observations of the specific solvation of primary amines (Figure 4), it seems appropriate to assign the cluster with $n = 40$ as having both protonated ornithines incorporated as part of pentagonal dodecahedron clathrates as shown in structure **4**.

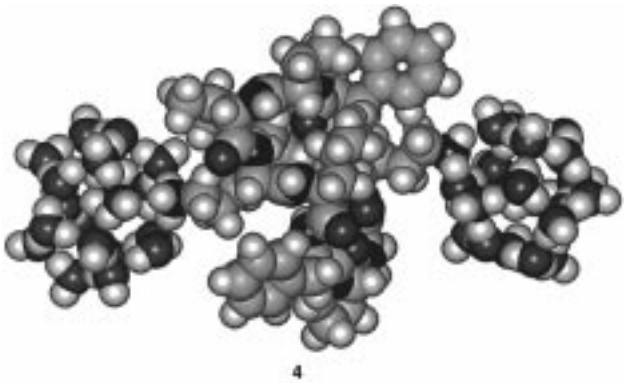

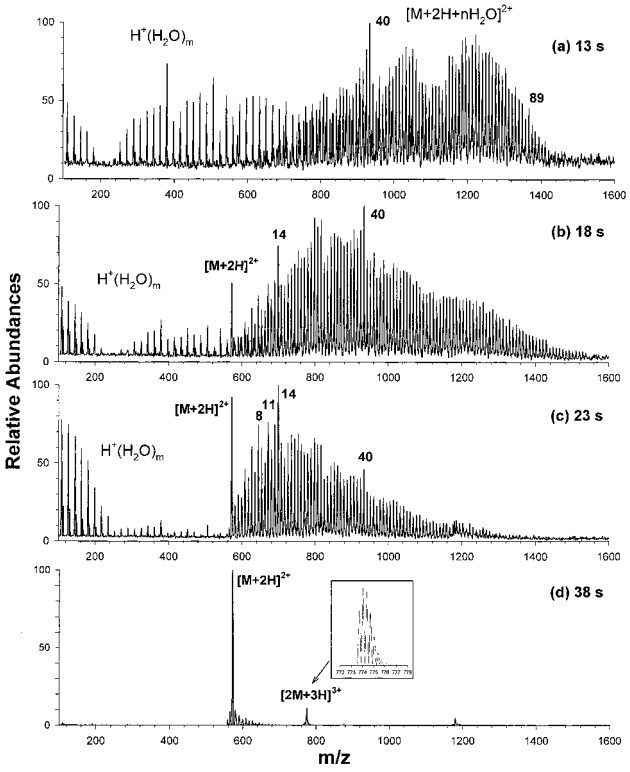

Figure 6. Water clusters of doubly protonated gramicidin S detected at various delay times. Sample concentrations are 50 μM in 0.01% acetic acid solution. Some magic number clusters are observed in the mass spectra with the $n = 40$ as the most prominent peak.

Both PM3 and molecular mechanics calculations with the use of universial force field[27] predict that the lowest energy structure of unsolvated doubly protonated gramicidin S has one protonated ornithine tucked into the ring, stabilized by hydrogen bond formation to the amide carbonyl oxygens (structure **5**). This structure is estimated to be approximately 20 kcal/mol more stable than one with both protonated ornithines extended as in **4**.

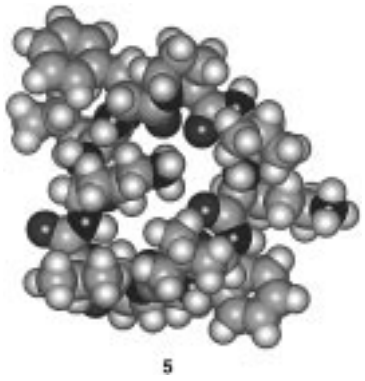

It is of interest that a magic number is not observed at $n = 20$, where the extended protonated ornithine in **5** is solvated in a pentagonal dodecahedron. Breakup and evaporation of water from the clathrate structures results from blackbody infrared excitation. The kinetics of this process may lead to nearly simultaneous rupture of the two clathrate structures in **4**. Alternatively, the breakup of one clathrate structure and subsequent solvation of the protonated ornithine by hydrogen bonding to the amide carbonyls as in **5** would lead to energy release which accelerates evaporation of water from the second

(27) (a) Rappe, A. K.; Casewit, C. J.; Colwell, K. S.; Goddard, W. A.; Skiff, W. N. *J. Am. Chem. Soc.* **1992**, *114*, 10024. (b) Rappe, A. K.; Goddard, W. A. *J. Phys. Chem.* **1991**, *95*, 3358.

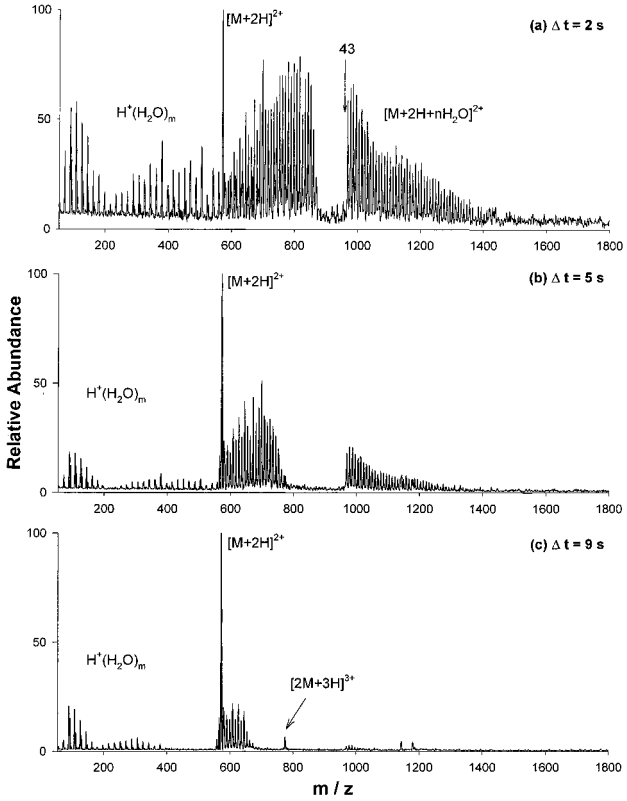

Figure 7. Water clusters of doubly protonated gramicidin S while a specific cluster ($n = 43$) is continuously ejected with various ejection times. No multiple loss of waters from the clusters is observed.

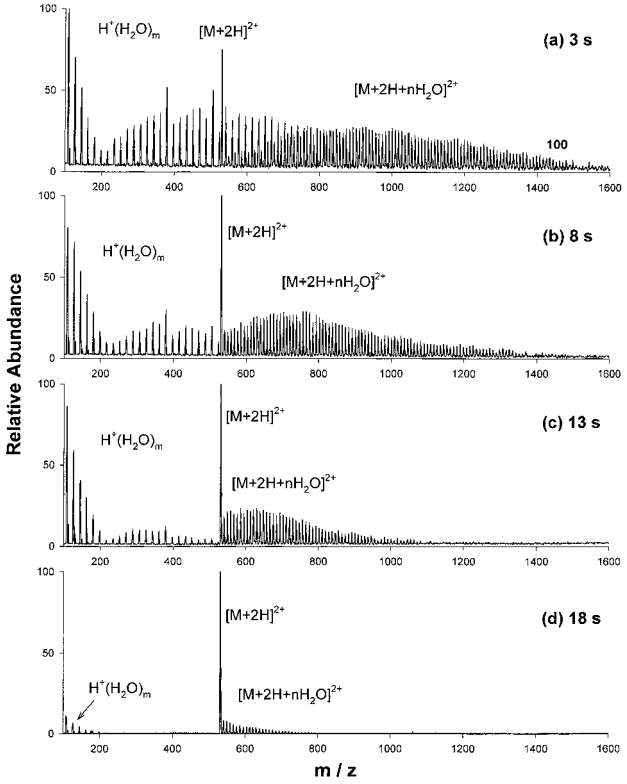

Figure 8. Water clusters of doubly protonated bradykinin detected at various delay times. Sample concentrations are 50 μM in 0.01% acetic acid solution. No specific solvation is observed.

clathrate. The structures associated with the magic numbers 8, 11, and 14, which have previously been noted in another study,[16] have no parallel in any simple model compounds that we have examined to date. They very likely represent specific solvation of **5** where the waters connect the protonated ornithines with other functional groups in the peptide.[16]

The possibility of the loss of small clusters of water molecules from highly solvated ions has been examined by ejecting a specific hydrated ion for extended times. One of these experiments is presented in Figure 7, which shows mass spectra of water clusters of doubly protonated gramicidin S when the $n = 43$ cluster is continuously ejected. At longer times, the gap in the distribution widens. The clusters observed in the gap in Figure 7a are identified as protonated water clusters. No water clusters of doubly protonated gramicidin S were observed in the gap, indicating that water evaporation occurs by sequential loss of single molecules. Similar studies with a wide range of cluster sizes gave identical results. Related experiments with the same conclusion have been reported by Bondybey and coworkers.[5]

Water Clusters of Doubly Protonated Bradykinin. Spectra of doubly protonated bradykinin (a nonapeptide Arg-Pro-Pro-Gly-Phe-Ser-Pro-Phe-Arg having terminal arginine residues as the sites of protonation) with more than 100 water molecules attached initially are shown at various detection delay times in Figure 8a−d. The cluster distribution is smooth with no prominent magic numbers. Water evaporation, nearly complete at 18 s, is more rapid than for species where clathrate formation or specific functional group solvation is observed. The delocalized charge distribution of protonated arginine reduces the hydrogen bonding capability of labile protons for these residues, and the molecular geometry does not facilitate incorporation of the functional group as part of a stable clathrate structure. Self-solvation of these protonated residues by the peptide chain may also mitigate specific solvation by water molecules.

Water Clusters of Singly and Doubly Protonated Diamines and Tetrabutylammonium Ion. Other experiments with a range of small molecules and peptides have revealed intriguing aspects of ion solvation and clathrate formation. Although incorporation of both functional groups into pentagonal dodecahedrons was anticipated, doubly protonated 1,12-diaminododecane does not exhibit any magic numbers (Figure 9a). In the low dielectric environment of the gas phase, it may be energetically more favorable for water to accumulate between the two charge centers to reduce the Coulombic repulsion rather than form clathrate structures at each end of the ion.

Another interesting result is shown in Figure 9b, where the tetrabutylammonium ion, with no labile protons available as strong hydrogen bonding sites, exhibits numerous prominent magic numbers. Since this ion is too bulky to be enclosed by the small clathrates, we believe that the magic numbers are associated with neutral clusters (e.g., for $n = 21$ and 28, the pentagonal dodecahedron (structure **6**) and pentakaidecahedron

6

encapsulate one and two neutral water molecules, respectively) which adhere to the spectator ion. The ion−cluster attraction is enhanced by the flexibility associated with the orientations of the water molecules in the cluster, making it possible for the

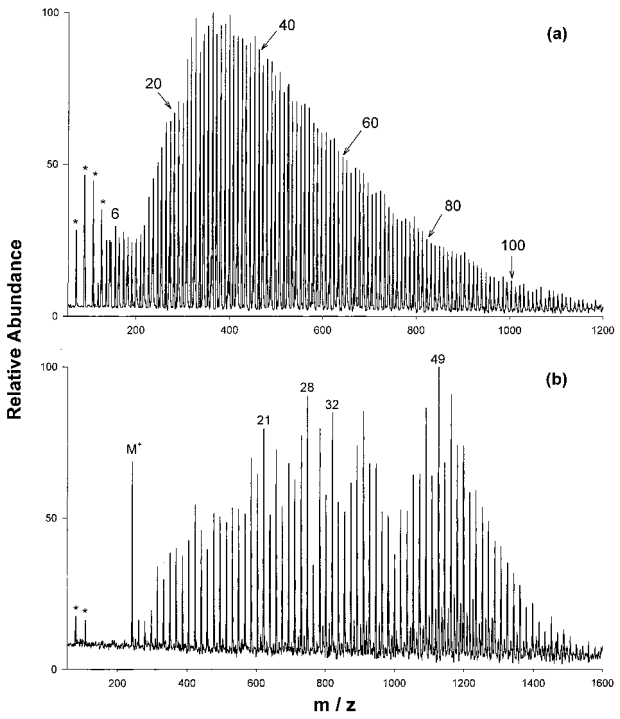

Figure 9. Water clusters of (a) doubly protonated 1,12-diaminododecane (23 s), and (b) tetrabutylammonium ion (10 s). Sample concentrations are approximately 100 μM in 0.01% acetic acid solution. The asterisks indicate protonated water clusters.

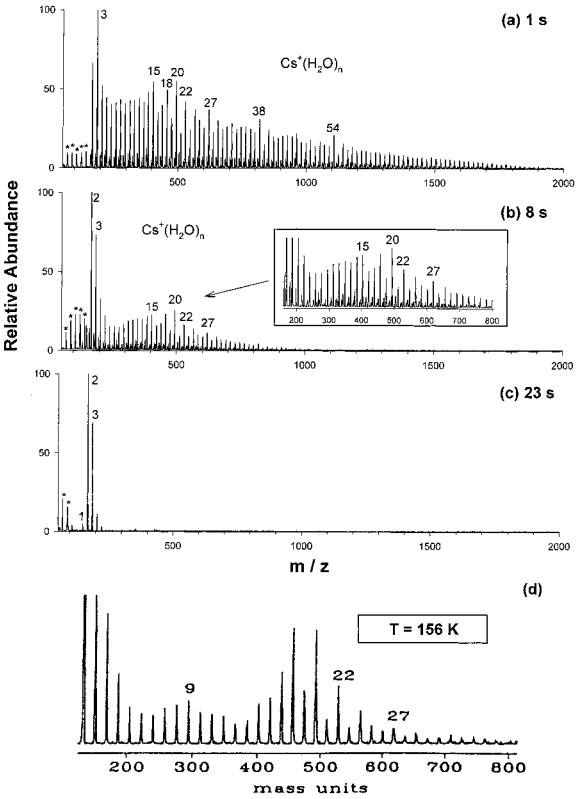

Figure 10. Water clusters of cesium ion generated by ESI and detected at various delay times (a−c). (d) Water clusters observed by Castleman and co-workers using flow tube technique. Cluster distribution detected at 8 s after ion production (inset of b) is remarkably similar to the one in d. The asterisks indicate protonated water clusters.

clathrates to have moderately high dipole moments (in the range 3−5 D as estimated by PM3 calculation). Recently, Courty et al. investigated water clusters of benzene and toluene cations using REMPI and observed magic numbers of 21 and 28 for $[Bz(H_2O)_n]^+$ and $[To(H_2O)_n]^+$ in reflectron time-of-flight mass spectra.[28] They suggested that the formation of protonated water clusters resulted from proton transfer from the aromatic radical cation to neutral water clusters. The present results with tetrabutylammonium ion indicate that they may have observed neutral clusters attached to the parent radical cations as spectator ions. We have not observed any instances where neutral clathrates appear to bind strongly to protonated peptides.

The possibility that such clusters might dissociate directly to the neutral clathrate and the spectator ion was investigated using a triple quadrupole mass spectrometer equipped with an electrospray ion source (API 365, Perkin-Elmer/Sciex). Specific size clusters were selected in the first quadrupole, and dissociation products were mass-analyzed with the third quadrupole using a range of pressures in the intermediate radio frequency only collision cell to effect dissociation. We observe that the clusters fragment by the sequential loss of single water molecules in analogy with the results of the FT-ICR ion ejection experiments described above.

Mechanism of Formation of Magic Number Clusters. The shape of the time dependent cluster distributions clearly reflects aspects of cluster stability and the desolvation dynamics which are not well understood at present, especially in the cases where specific solvation of the core ion is observed. Molecules with functional groups that interact strongly with solvent may be in an extended configuration when surrounded by solvent. As solvent evaporation proceeds, the molecule folds to derive advantage from intramolecular solvation of charged functional groups. As a result, evaporative cooling is not as effective since intermolecular solvation is being replaced by intramolecular interactions. Molecules that are already folded in solution to form a hydrophobic globular species will not exhibit this effect. Charged functional groups that do not benefit from intramolecular solvation, especially hydrogen bonding sites, may interact strongly with a small number of water molecules, which evaporate slowly in comparison to larger clusters. Water molecules that are an integral component in a stable structure may similarly be identified by their persistent binding, which in turn might suggest gas-phase structures not unlike those in condensed phase.

Questions arise with respect to the mechanism of formation of stable water clusters. There are two fundamentally different approaches to formation of clathrates. When clusters are built up by sequential binding of individual water molecules, as in the studies reported by Castleman and co-workers,[29] each addition results in heating and concomitant annealing of growing clusters. This is distinctly different from the process of solvent evaporation since water loss is a cooling mechanism. However, the accumulation of sufficient internal energy to produce dissociation requires internal energy sufficient to also produce annealing. Figure 10 shows FT-ICR results for water clusters of cesium ion at various detection delays along with the cluster distribution observed earlier by Castleman and co-workers[29] (Figure 10d) in their flow system at 156 K. The cluster size distributions resulting from the two distinct approaches are remarkably similar, especially in the region $n = 18-29$ measured at a delay time of 8 s (Figure 10b). This may indicate that stable clathrates are not necessarily present in larger frozen clusters, preserved as snapshots of instantaneous water structures

(28) Courty, A.; Mons, M.; Le Calve, J.; Piuzzi, F.; Dimicoli, I. *J. Phys. Chem. A* **1997**, *101*, 1445.

(29) Selinger, A.; Castleman, A. W., Jr. *J. Phys. Chem.* **1991**, *95*, 8442.

that are then revealed by the evaporation process. Rather, they may be formed from a specific number of water molecules as a result of annealing processes. It is of interest to address these issues with molecular dynamics simulations. Recently, Monte Carlo studies of the structure and thermodynamics of $H^+(H_2O)_n$ clusters by Svanberg and Petterson[30] show that $H^+(H_2O)_{21}$ attains a dodecahedral cage configuration at temperature below 150 K and that the structure does not survive above 170 K. They conclude that magic number behavior is restricted to temperatures below the melting point of the cluster.

Conclusions

Appropriate operation of an electrospray ion source facilitates the formation of extensively hydrated molecular ions. Initial rapid loss of water results in evaporative cooling of clusters to temperatures around 130−150 K, and subsequent water loss reveals cluster size distributions with structures of special stability, drawing attention by their unusual abundance. These clusters are referred to as magic numbers, a terminology not inconsistent with the speculation they inspire regarding their structures. Armed with the desire to perpetuate historical perspective, the beauty of nature expressed in symmetry, and the feeble support added by semiempirical calculations, we propose that hydrated protonated primary amines form water clathrates where the protonated amine replaces a water molecule in one of the known water clathrate structures, with varying numbers of neutral water molecules encapsulated (e.g., 3). By extrapolation, this conjecture explains magic numbers observed for multiply protonated peptides with pendant primary amines, such as gramicidin S.

We are currently extending the present studies to encompass a broad range of ionic species, focusing on an examination of the specific solvation of functional groups in biopolymers. In addition, the observation of neutral clathrates attached to spectator ions such as the tetrabutylammonium ion presages a range of studies of the encapsulation of small molecules in clathrate structures. The addition of neutral molecules either in the ESI source capillary or in the ICR cell may lead to their incorporation within the clathrate structures. An exact fit may be signaled by specially enhanced cluster stability. Finally, the interaction of neutral molecules with ionic water clusters is being examined to explore the intriguing possibility of observing chemical processes with reaction conditions which bridge the gap between solution and the gas phase.

Acknowledgment. This work was supported in part by the National Science Foundation under Grant CHE-9727566. We gratefully acknowledge the financial support of P.F. from the Swiss National Science Foundation and the Ciba-Geigy Jubilee Foundation, and of T.S. from the Deutsche Forschungsgemeinschaft (DFG). Funds for instrument development have also been provided by ARPA and the DOD-URI program (ONR-N0014-92-J-1901). We are indebted to the Beckman Foundation and Institute for the initial funding and continuing support of the research facilities. We also thank Dr. Gary M. Hathaway and Dr. Jie Zhou at the Protein/Peptide Micro Analytical Laboratory (PPMAL) of the Beckman Institute for helping to acquire the triple quadrupole mass spectral data.

JA982075X

(30) Svanberg, M.; Pettersson, J. B. C. *J. Phys. Chem. A* **1998**, *102*, 1862.